Spatial dependence of the pairing field calculated with bare and induced interactions

A Pastore[1], F Barranco[2], RA Broglia[3,4,5] and E Vigezzi[3]

[1] Department of Physics, Post Office Box 35 (YFL), FI-40014 University of Jyväskylä, Finland
[2] Departamento de Fisica Aplicada III, Escuela Superior de Ingenieros, Camino de los Descubrimientos s/n, 41092 Sevilla, Spain.
[3] INFN, Sezione di Milano, via Celoria 16, 20133 Milano, Italy.
[4] Dipartimento di Fisica, Università degli Studi di Milano,via Celoria 16, 20133 Milano, Italy.
[5] The Niels Bohr Institute, University of Copenhagen, Blegdamsvej 17, 2100 Copenhagen Ø, Denmark.

Abstract. The interaction induced by the exchange of low-lying surface vibrations between pairs of orbitals close to the Fermi surface provides an important contribution to pairing correlations in superfluid nuclei. We study the spatial dependence of the pairing field obtained adding the bare and induced interaction in ^{120}Sn.

1. Introduction

The superfluid properties of nuclear systems are strongly influenced by polarization phenomena. In particular, the exchange of low-lying surface vibrations between pairs of nucleons close to the Fermi surface gives rise to an attractive induced interaction, that accounts for about one half of the value of the pairing gap derived from the experimental odd-even mass differences in superfluid nuclei [1]. If one wants to obtain a consistent calculation of the gap, one must add the effects of the nucleon-nucleon interaction, and take into account the self-energy and vertex processes that renormalize the quasiparticle strength and increase the level density around the Fermi energy. It has been shown that this procedure leads to gaps in reasonable agreement with experiment, if one starts from a single-particle spectrum associated with a $k-$effective mass $m_k \sim 0.7$, like that obtained in a Hartree-Fock calculation with the SLy4 force [2].

In this paper we study the pairing gap in coordinate space. Because our study aims at determining the basic features of the spatial dependence of the gap, rather than its precise magnitude, use is made of approximations to deal with some of these effects, in particular with self-energy effects, so as to gain in transparency in the presentation of the results. In order to make contact with other, more phenomenological approaches available in the current literature, we shall parametrize our results in terms of a density dependent, zero-range interaction.

2. The pairing induced interaction

We start by performing a Hartree-Fock calculation with the two-body interaction SLy4, obtaining a set of single-particle energy levels e_{nlj}. We then use this basis to solve the Hartree-Fock-Bogoliubov (HFB) equations in the pairing channel. The calculations are performed in a spherical box of radius $R_{box} = 15$ fm. For more details we refer to [3].

The matrix elements of the interaction induced by the exchange of a vibration will be calculated using the formalism already employed in Ref. [4]:

$$\langle \nu_1' m' \nu_2' \bar{m}' | v_{ind} | \nu_1 m \nu_2 \bar{m} \rangle =$$

$$\sum_{J^\pi M i} \frac{(f+g)^{\nu_1' m'}_{\nu_1 m; J^\pi M i}(f-g)^{\nu_2' m'}_{\nu_2 m; J^\pi M i}}{E_0 - (|e_{\nu_1'} - e_F| + |e_{\nu_2} - e_F| + \hbar\omega_{J^\pi i})} + \sum_{J^\pi M i} \frac{(f+g)^{\nu_1' m'}_{\nu_1 m; J^\pi M i}(f-g)^{\nu_2' m'}_{\nu_2 m; J^\pi M i}}{E_0 - (|e_{\nu_1} - e_F| + |e_{\nu_2'} - e_F| + \hbar\omega_{J^\pi i})}. \quad (1)$$

The index i labels the exchanged vibrational modes, having angular momentum and parity $J^\pi M$ and energy $\hbar\omega_{J^\pi i}$. The modes have been calculated in the Quasiparticle Random Phase Approximation (QRPA), using the same interaction already employed to calculate the mean-field, with the exception of the spin-orbit and of the Coulomb part [5]. E_0 is the pairing correlation energy of a Cooper pair, a quantity which is of the order of $-2\Delta_F$, where Δ_F is the average value of the gap close to the Fermi energy. In Eq. (1) f and g denote the particle-vibration coupling vertices associated with the spin-independent and spin-dependent parts of the residual interaction:

$$v_{ph}(\vec{r}, \vec{r}') = \delta(\vec{r} - \vec{r}') \times \left\{ \left[F_0(r) + F_0'(r)\vec{\tau} \cdot \vec{\tau}' \right] + \left[\left(G_0(r) + G_0'(r)\vec{\tau} \cdot \vec{\tau}' \right) \vec{\sigma} \cdot \vec{\sigma}' \right] \right\}, \quad (2)$$

where F_0, F_0' (G_0, G_0') are the generalized Landau-Migdal parameters associated with the SLy4 force controlling the isoscalar and isovector spin-independent (spin-dependent) channels. In the calculation of the particle-vibration coupling we neglected the momentum-dependent part of the interaction (this part is instead taken into account in the QRPA calculation). The vertex f is given by

$$f^{\nu' m'}_{\nu m; J^\pi M i} = i^{l - l'} \langle j' m' | (i)^J Y_{JM} | j m \rangle \times$$

$$\int dr \varphi_{\nu'} [(F_0 + F_0')\delta\rho^i_{J^\pi n} + (F_0 - F_0')\delta\rho^i_{J^\pi p}]\varphi_\nu. \quad (3)$$

The quantities $\delta\rho^i_{J^\pi n}$ and $\delta\rho^i_{J^\pi p}$ are the neutron and proton contributions to the transition densities and are given by

$$\delta\rho^i_{J^\pi}(r) = \frac{1}{\sqrt{2J+1}} \sum_{\nu_1, \nu_2} (X_{\nu_1, \nu_2}(i, J^\pi) + Y_{\nu_1, \nu_2}(i, J^\pi)) \times$$

$$(u_{\nu_1} v_{\nu_2} + u_{\nu_2} v_{\nu_1}) \langle \nu_1 || i^J Y_J || \nu_2 \rangle \varphi_{\nu_1}(r) \varphi_{\nu_2}(r), \quad (4)$$

where u_{ν_1} and v_{ν_1} are the quasiparticle amplitudes and X_{ν_1, ν_2} and Y_{ν_1, ν_2} denote the forward and backward amplitudes of the QRPA modes. The vertex g is given by a similar expression, substituting F_0, F_0' with G_0, G_0' [4].

3. Pairing gap in coordinate space

Solving the HFB equations in the pairing channel with the induced interaction (1) we obtain the matrix elements of the state-dependent pairing gap $\Delta_{nn'lj}$: the diagonal ones are shown below in figure 4(a). We can then derive the pairing field in position space $\Delta(\vec{r}, \vec{r}')$ [3]. This is shown in figure 1(a) as a function of the center of mass $R_{c.m.}$ and of the relative distance r_{12} of the pair, after averaging over the angle between $\vec{R}_{c.m.}$ and $\vec{r}_{12}$. For a given value of r_{12} the pairing field has a maximum close to the surface of the nucleus ($R_{c.m.} \sim 6$ fm), while it becomes negative in the interior, essentially due to the repulsive interaction induced by the exchange of spin modes, associated with the G_0, G_0' terms of the residual interaction (2). Taking the Fourier transform with respect to the relative distance $\vec{r}_{12}$, we can define the pairing field in momentum space

$$\Delta(\vec{R}_{c.m.}, \vec{k}) = \int d^3 r_{12} \Delta(\vec{r}, \vec{r}') \exp^{-i\vec{k} \cdot \vec{r}_{12}}, \quad (5)$$

which is shown in figure 1(b) after averaging over the angle between $\vec{R}_{c.m.}$ and $\vec{k}$. We now consider the pairing gap obtained adding the matrix elements of the bare Argonne v_{14} nucleon-nucleon interaction v_{Arg}. We can also take into account self-energy effects in a simplified way, multiplying the total interaction $v_{Arg} + v_{ind}$ by a factor $Z = 0.7$, which is the typical value of the quasiparticle strength calculated for levels around the Fermi energy [6]:

$$v_{Arg+ind} = Z(v_{Arg} + v_{ind}). \tag{6}$$

While the pairing matrix elements are reduced by a factor Z^2, they are also enhanced by a factor $1/Z$ due to the increase in the density of levels; hence the overall multiplying factor Z [7].
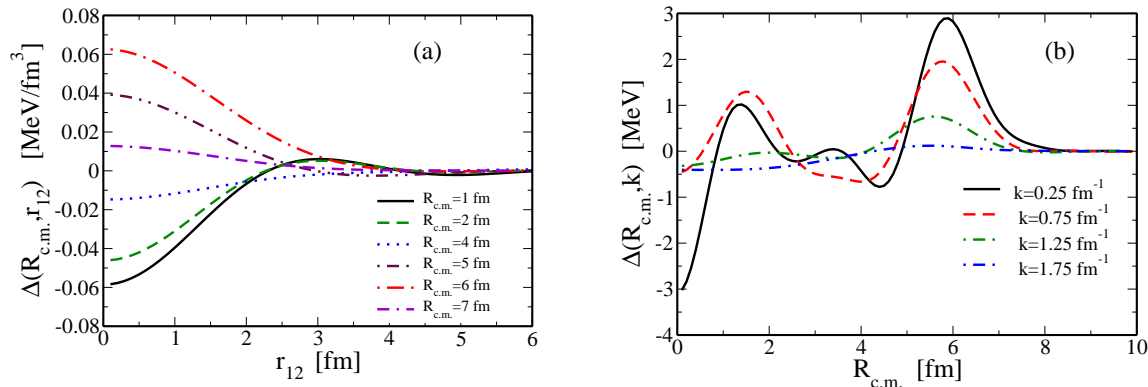

Figure 1. Pairing field in position space (a), and in momentum space (b) obtained with the induced interaction v_{ind}.

The diagonal matrix elements of the pairing gap Δ_{nnlj} obtained with the interaction $v_{Arg+ind}$ are shown below in figure 4(b) and 5(b). They correspond to a value $\Delta_F = 1.32$ MeV, obtained averaging over the single-particle levels located within an interval of ± 2 MeV around the Fermi energy (note that the value reported in [3] is about 10% larger, due to a numerical error in the calculation of some matrix elements of the induced interaction). This value is in good agreement with that derived from the empirical odd-even mass difference, but one should keep in mind that the magnitude of the gap is sensitive both to the adopted value of Z and to the effective mass of the mean field. To better assess the spatial structure of the pairing field, we prefer to introduce a local approximation [8, 9]. We define $\Delta_{loc}(R_{c.m.}) \equiv \Delta(R_{c.m.}, k_F(R_{c.m.}))$, where $k_F(R_{c.m.})$ is the local Fermi momentum. In figure 2(a) we compare the results obtained using the bare interaction and the bare plus induced interaction (6). The bare interaction leads to a peak at the surface, which is reinforced by the induced interaction. The induced interaction also produces a negative gap in the interior of the nucleus, in keeping with the results shown in figure 1.

The local approximation introduced above, based on the results obtained in the microscopic HFB calculation, leads to pairing gaps which are rather different from those obtained from the simplest Local Density Approximation, which does not take into account proximity effects associated with the nuclear surface and the fact that the nuclear radius is smaller than the coherence length in uniform matter. This can be seen in figure 2(b), where we compare the local pairing gap Δ_{loc} associated with the Argonne interaction only, with the function $\Delta_{LDA}(R_{c.m.}) = \Delta_F^{n.m.}(\rho_n(R_{c.m.}))$, where $\Delta_F^{n.m.}$ is the pairing gap calculated with the Argonne interaction at the Fermi energy in uniform neutron matter, for a density equal to the neutron density at a distance $R_{c.m.}$ from the center of the nucleus, and using the local value of the
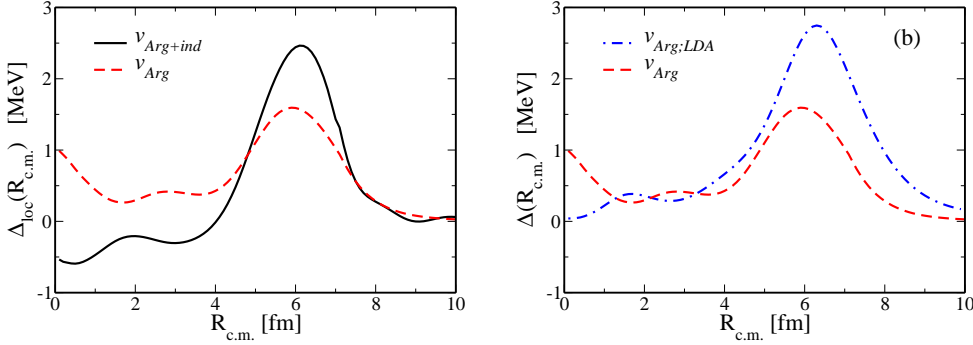
Figure 2. (a) Local pairing gaps calculated in ^{120}Sn with the interactions v_{Arg} (dashed line) and $v_{Arg+ind}$ (solid line). (b) The local pairing gap calculated with v_{Arg}, already shown in (a), is compared to the gap obtaining using the simple LDA approximation based on the pairing gap calculated with the Argonne interaction in uniform matter (solid line).

effective mass. The LDA overestimates the difference between the pairing gap on the surface and in the interior of the nucleus.

4. Parametrization of the pairing interaction

4.1. Finite range parametrization

We now introduce a parametrization of the induced interaction, v_{ind}, based on the surface or volume character of the interaction associated with the spin-independent or the spin-dependent part of the matrix elements (1). We try to determine a Gaussian function $v_{ind}^G(R_{c.m.}, r_{12})$ so as to fulfill approximately the relation

$$\Delta(R_{c.m.}, r_{12}) = -v_{ind}^G(R_{c.m.}, r_{12})\Phi^{S=0}(R_{c.m.}, r_{12}), \tag{7}$$

where $\Phi^{S=0}(R_{c.m.}, r_{12})$ is the abnormal density in the $S = 0$ channel, the dominant one. We consider separately the contributions from the attractive. spin-independent and from the repulsive, spin-dependent parts of the interaction writing $v_{ind}^G(R_{c.m.}, r_{12}) = v_{attr}^G(R_{c.m.}, r_{12}) + v_{rep}^G(R_{c.m.}, r_{12})$. We shall first fit the pairing gap obtained including only the spin-independent part of v_{ind} (that is, putting $G = G' = 0$ in Eq.(2)), using the function

$$v_{attr}^G(R_{c.m.}, r_{12}) = -b_{attr} \cdot \exp\left(-[(r_{12} - c)/a_{attr}]^2\right) \tag{8}$$

where a_{attr}, b_{attr}, c are parameters to be determined. We fix c so as to constrain the Gaussian function to be maximum when at least one of the neutrons is on the surface of the nucleus. This implies $c = |R_{nucl} - R_{c.m.}|$, where R_{nucl} is the maximum of the first derivative of the self-consistent single-particle potential. The parameter a_{attr} turns out to be close to $a_{attr} \approx 2$ fm, so in practice to simplify the fitting method we used the fixed value $a_{attr} = 2$ fm. The resulting values of the parameter b_{attr} obtained as a function of $R_{c.m.}$ are peaked on the nuclear surface and are plotted in figure 3(a).

The repulsive part of the induced interaction is active only in the interior of the nucleus, say for $R_{c.m.} \leq 4.5$ fm (cf. figure 1(a)), so we multiply the Gaussian by a Heaviside function centered at $R_0 = 4.5$ fm

$$v_{rep}^G(R_{c.m.}, r_{12}) = b_{rep}\exp\left(-[r_{12}/a_{rep}]^2\right)\Theta(R_{c.m.} - R_0). \tag{9}$$
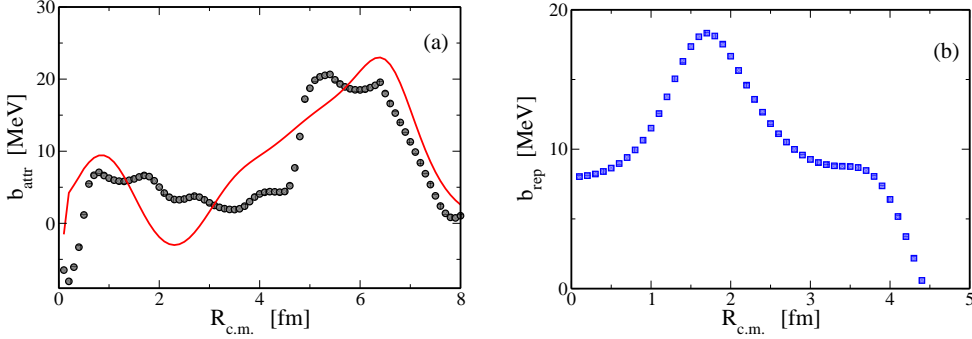
Figure 3. (a) The values of the parameter b_{attr}, obtained fitting the Gaussian interaction (cf. Eq.(8)) for ^{120}Sn, are shown as a function of the center of mass $R_{c.m.}$ (filled dots), and are compared with the function $dU(R_{c.m.})/dR_{c.m.}$ (solid line). (b) The values of the parameter b_{rep}, obtained fitting the Gaussian interaction Eq. (10), are also shown as a function of the center of mass $R_{c.m.}$ (filled squares).

Table 1. Average gaps and pairing energies (in MeV) obtained with the full expression (1) of the induced interaction and with the Gaussian parametrization v_{ind}^G.

Nucleus	Δ_F^{full}	Δ_F^G	E_{pair}^{full}	E_{pair}^G
^{108}Sn	1.02	1.07	-4.02	-5.77
^{112}Sn	1.87	1.65	-9.67	-11.20
^{116}Sn	1.34	1.18	-6.74	-7.72
^{120}Sn	0.88	0.96	-5.98	-5.85

We then determine the parameters of the repulsive Gaussian, fitting the values of a_{rep}, b_{rep} so that the resulting interaction

$$v_{ind}^G(R_{c.m.}, r_{12}) = v_{attr}^G(R_{c.m.}, r_{12}) + v_{rep}^G(R_{c.m.}, r_{12}) \tag{10}$$

satisfies Eq.(7) for values of r_{12} in the interval [0,2] fm, where we used in this case the gaps $\Delta(R_{c.m.}, r_{12})$ and the abnormal density $\Phi^{S=0}(R_{c.m.}, r_{12})$ obtained from the full calculation of the induced interaction considering both spin modes and density modes. The parameter a_{rep} turns out to be very close to $a_{rep} \approx 3.5$ fm, so in practice we used a fixed value $a_{rep} = 3.5$ fm. In figure 3(b) we show the resulting values of b_{rep} as a function of $R_{c.m.}$.

We found that it is possible to parametrize b_{attr} as $b_{attr} \sim \beta_{attr} R_{nucl} \frac{dU(R_{c.m.})}{dR_{c.m.}}$. The resulting values of β_{attr} for $A = 108, 112, 116$ and 120 are $\beta_{attr}= 0.157, 0.172, 0.163$ and 0.154 respectively.

The Gaussian parametrization gives pairing gaps and pairing energies in good agreement with the original induced interaction (1), as shown in table 1. We can then insert it in Eq. (6) in place of v_{ind}, and calculate the pairing gap associated with the bare plus induced interaction. For the case of ^{120}Sn we obtain $\Delta_F^G = 1.47$ MeV and $E_{pair}^G = -17.52$ MeV to be compared with $\Delta_F = 1.32$ MeV and $E_{pair} = -13.98$ MeV obtained with the original induced interaction (cf. table 2).
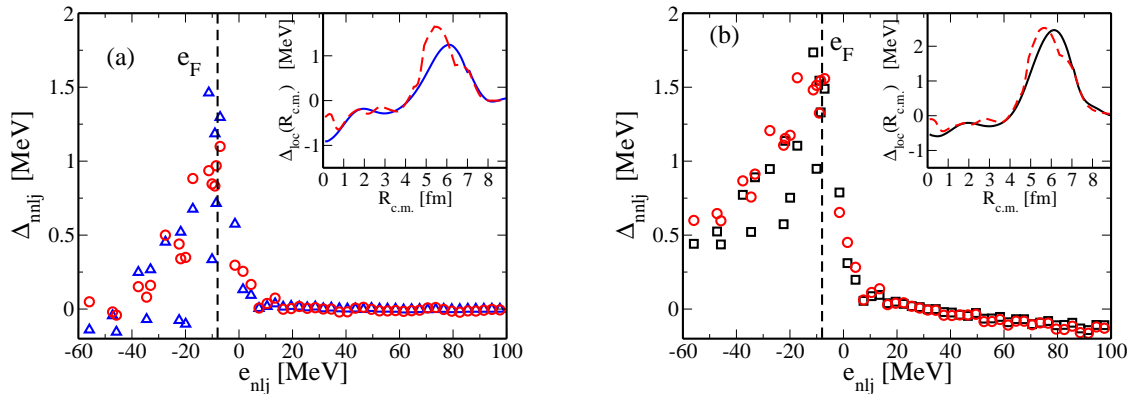
Figure 4. (a) The diagonal matrix elements of the pairing gap in ^{120}Sn, associated with the induced interaction v_{ind} (triangles), are compared with those associated with the Gaussian parametrization (circles, cf. Eq. (10)). The spatial dependence of the semiclassical pairing gap associated with the induced interaction (solid line) and with the Gaussian interaction (dashed line) are shown in the inset. (b) The same, but for the Argonne plus induced interaction.

4.2. DDDI parametrization

The local pairing fields discussed in Section 3 can be compared to those obtained by several authors, who employed a density-dependent pairing interaction (DDDI) of the form [10]-[14]:

$$v^{\delta}(\vec{r}_1, \vec{r}_2) = v_0 \left[1 - \eta \left(\frac{\rho\left(\frac{\vec{r}_1+\vec{r}_2}{2}\right)}{\rho_0} \right)^{\alpha} \right] \delta(\vec{r}_1 - \vec{r}_2), \tag{11}$$

where ρ_0 is the nuclear saturation density and v_0, η, α are three parameters to be determined, together with the value of a cutoff energy in the single-particle energies E_{cut}, needed to solve the HFB equations with a zero-range interaction. The parameter v_0 together with E_{cut} defines the strength of the pairing interaction, while the other two parameters determine the shape of the pairing field. For a given value of E_{cut}, the strength can be fixed at zero density so as to reproduce the neutron scattering length. We shall use the single-particle levels which lie up to 60 MeV above the Fermi energy, following Ref. [15], and we shall put $v_0 = -458.4$ MeV fm^3 accordingly.

The parameters α and η have been determined in previous works either to reproduce experimental gaps or to reproduce the pairing gap at the Fermi energy obtained with a finite range interaction like Gogny or Argonne in uniform neutron matter. In this section we want instead to determine the parameters of the DDDI from the condition that the spatial dependence of the associated gaps reproduces the spatial dependence of the local pairing fields determined in the previous section. We fit the parameters η and α, minimizing the deviation between the form of the pairing gap obtained with the DDDI of Eq. (11) and the form of the gap obtained with the local potentials. We note that if an interaction has positive values for $R_{c.m.} = 0$ the parametrization (cf. Eq.(11)) implies that $\eta > 1$. For a given value of η, the larger the value of α, the more attractive the interaction is on the surface, leading to larger values of the gap. Imposing a given value Δ_F for the average pairing gap, one obtains a relation between α and η, shown in the inset of figure 6(a) for various values of Δ_F: the spatial dependence of the pairing gaps obtained for various values of α when $\Delta_F = 1.3$ MeV is also shown in figure 6(a).
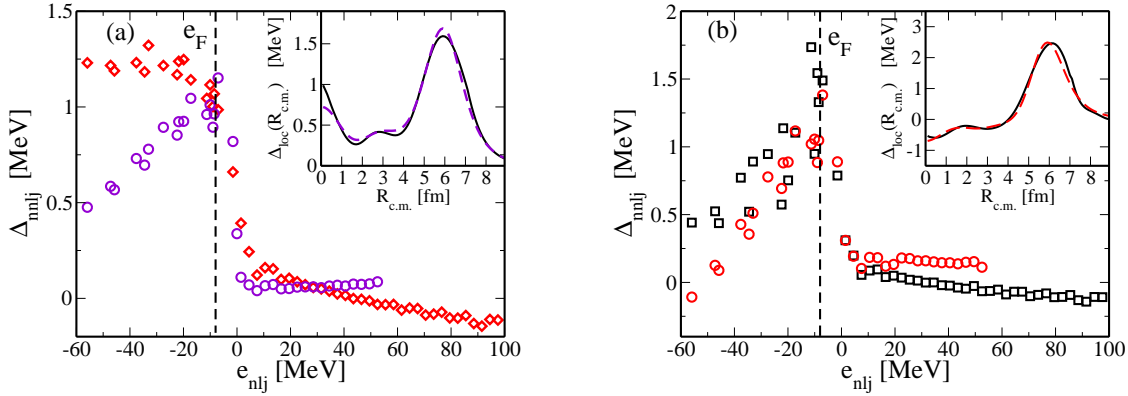
Figure 5. (a) The diagonal matrix elements of the pairing gap associated with the Argonne interaction v_{Arg} (diamonds) are compared with those associated with the DDD, zero-range interaction with the parameters $\alpha = 0.66$, $\eta = 0.84$ (circles). The local pairing gaps associated with the Argonne interaction (solid line) and with the zero-range interaction (dashed line) are shown in the inset. (b) The same, for the Argonne+induced interaction $v_{Arg+ind}$ compared with the DDDI with the parameters $\alpha = 1.5$, $\eta = 1.15$ (circles, cf. table 2).

The values of the parameters for v^{δ}_{Arg} and $v^{\delta}_{Arg+ind}$, calculated for ^{120}Sn, are reported in table 2, while the resulting fits are shown in the insets of figures 5(a) and 5(b). While the spatial dependence of the local gaps is quite well reproduced, the diagonal matrix elements of the pairing gaps, shown in figure 5 and the pairing energy (reported in table 2) are underestimated, especially in the case of the total interaction $v^{\delta}_{Arg+ind}$. The values of the parameters for the Argonne interaction are very close to those obtained by Matsuo for the bare interaction in uniform neutron matter [15]. We extended the analysis for the bare interaction to the nuclei $^{102-130}$Sn and $^{36-46}$Ca, finding $\bar{\alpha} = 0.67 \pm 0.04, \bar{\eta} = 0.82 \pm 0.05$, showing that the parameters given in table 2 are quite stable.

In figure 6(b) we compare the spatial dependence of the three DDD interactions listed in table 2. By construction, all interactions tend to the value $v_0 = $ -458.4 MeV fm^{-3} for large values of $R_{c.m.}$. The bare+induced interaction $v^{\delta}_{ind+Arg}$ is considerably more attractive than the bare

Table 2. Parameters of the DDDI, Eq. (11), producing pairing gaps which fit the local semiclassical pairing fields obtained with the various interactions. In the last four columns we compare the pairing gap at the Fermi energy and the pairing energies (in MeV) obtained with the full calculation, Δ_F^{full} and E_{pair}^{full}, with the values obtained using the corresponding density dependent interaction, Δ_F^{δ} and E_{pair}^{δ}.

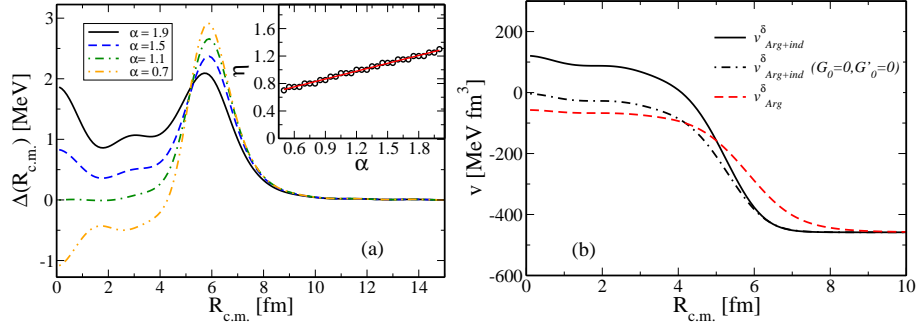| Interaction	α	η	Δ_F^{full}	Δ_F^{δ}	E_{pair}^{full}	E_{pair}^{δ}
v^{δ}_{Arg}	0.66	0.84	1.04	1.03	-13.2	-8.9
$v^{\delta}_{Arg+ind}$	1.5	1.15	1.32	1.09	-13.98	-11.78
$v^{\delta}_{Arg+ind}(G_0 = G'_0 = 0)$	1.38	0.91	2.12	1.85	-24.45	-25.68

Figure 6. (a) We show in the inset the linear relation between the parameters α and η in Eq.(11) obtained requiring that $\Delta_F = 1.3$ MeV, and in the main figure the resulting pairing gaps associated with specific values of α. (b) The three pairing interactions associated with the values of the parameters α and η given in table 2.

Argonne interaction in the surface region ($R_{c.m.} \sim 6$ fm). On the other hand, $v^{\delta}_{ind+Arg}$ has a repulsive character in the interior of the nucleus, which is caused by the exchange of spin modes, as can be seen setting G_0, G'_0 to zero.

5. Conclusions

We have presented a microscopic approach to the calculation of pairing correlations in superfluid nuclei, adding a bare nucleon-nucleon interaction and an induced interaction which takes into account the exchange of RPA vibrational modes, including self-energy effects in a simplified way. The resulting interaction is surface peaked, in keeping with the fact that the bare interaction is mostly attractive for low values of relative momentum, and that the exchange of collective surface modes gives the largest contribution to the induced interaction at the nuclear surface.

References

[1] Barranco F, Broglia RA, Gori G, Vigezzi E, Bortignon PF and Terasaki J 1999 *Phys. Rev. Lett.* **83** 2147
[2] Barranco F, Broglia RA, Colò G, Gori G, Vigezzi E and Bortignon PF 2004 *Eur.Phys.J.* A **21** 57
[3] Pastore A, Barranco F, Broglia RA and Vigezzi E 2008 *Phys. Rev.* C **78** 024315
[4] Gori G, Ramponi F, Barranco F, Bortignon PF, Broglia RA, Colò G and Vigezzi E 2005 Phys. Rev. C **72** 011302(R)
[5] Colò G and Bortignon PF 2001 *Nucl. Phys.* A **696** 427. Pairing correlations have been calculated in the BCS approximation with a simple seniority force, adjusted to the experimental pairing gap of ^{120}Sn.
[6] Terasaki J, Barranco F, Broglia RA and Vigezzi E 2002 *Nucl. Phys.* A **697** 127
[7] Barranco F, Bortignon PF, Broglia RA, Colò G, Schuck P, Vigezzi E and Viñas X 2005 *Phys. Rev.* C **72** 054314
[8] Ring P and Schuck P 2005 *The nuclear many-body problem* (Berlin: Springer)
[9] Barranco F, Broglia RA, Esbensen H and Vigezzi E 1998 *Phys. Rev.* C **58** 125
[10] Bertsch GF and Esbensen H 1991 *Ann. Phys. (N.Y.)* **209** 327
[11] Garrido E, Sarriguren P, Moya de Guerra E and Schuck P 1999 *Phys. Rev.* C **60** 064312
[12] Dobaczewski J, Nazarewicz W and Reinhard PG 2001 *Nucl. Phys.* A **693** 361
[13] Dobaczewski J, Nazarewicz W and Stoitsov MV 2002 *Eur. Phys. J.* A **15** 21
[14] Bertsch GF, Bertulani CA, Nazarewicz W, Schunk N and Stoitsov MV 2009 *Phys Rev.* C **79** 034306
[15] Matsuo M 2006 *Phys. Rev.* C **73** 04430.